PRAMANA
—journal of
physics

Vol. 53, No. 1,
July 1999
pp. 107–119

The lamellar and sponge phases of dilute surfactant systems: Structures and defects at equilibrium and under shear

MAURICE KLEMAN
Laboratoire de Mineralogie-Cristallographie (UMR CNRS 7590), Universites Paris VI et Paris VII, case 115, 4 place Jussieu, 75252 PARIS Cedex 05, France

Abstract. We report on the physical properties of swollen solutions of the amphiphilic molecules of cetylpyridinium chloride and hexanol in brine. A remarkable characteristic of this system is the existence of a crossover between dilute and less dilute solutions, in the lamellar phase and the sponge phase, with some interesting consequences for the theory of membranes.

Keywords. Lamellar and sponge phases; surfactants; defects.

PACS Nos 68.10.m; 47.20.Hw

1. Introduction

The swollen quasi-ternary surfactant system made of CpCl (cetylpyridinium chloride), hexanol and brine (1 % wt NaCl) displays a sequence of phases (micellar L_1, lamellar L_α, sponge L_3; see figure 1) whose stabilities are tuned by the bending modulus κ and the saddle-splay modulus $\bar{\kappa}$, as in other likewise swollen membrane systems: SDS (sodium decylsulphate), decanol and oil and/or brine; AOT (sodium sulpho-di (2-ethyloxyl) succinic ester), brine; etc.

Figure 2 shows a simplified version of the phase diagram [1] of the system that we are considering: $\phi_s = \phi_c + \phi_h$ is the total weight fraction of surfactant (ϕ_c, CpCl) and cosurfactant (ϕ_h, hexanol), $\phi_b = 1 - \phi_s$ is the brine weight fraction.

However this system also presents some characteristics which have not yet been documented in other swollen surfactants:

(a) An important, not yet fully explained, feature of the L_α phase samples observed at rest, is that the nature of the defects depends on the dilution [2]. More specifically, at constant composition of the membrane ($\phi_s/\phi_c = \text{const.}$): in the more dilute part of the L_α domain, most of the defects are spherulites (packings of spherical bilayers in the form of onions), while in the less dilute part Friedel's oily streaks [3] are present, most frequently split into classic focal conic domains (FCD's; see ref. [2b]).

(b) The shear experiments conducted in the L_α phase (lamellar phase) match rather closely with the phase diagram (established at rest, shear rate $\omega = 0$), in the sense that there is a stationary state of shear, with a spherulitic texture in the region where spherulites are observed at rest, and with other textures of defects in the region where

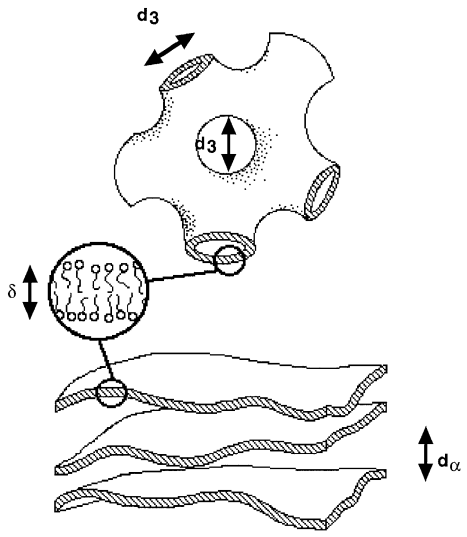

Figure 1. Schematic structures of the lamellar L_α and sponge L_3 phases. The characteristic lengths are indicated. Note also the typical shape of the sponge phase, made of 'passages'.

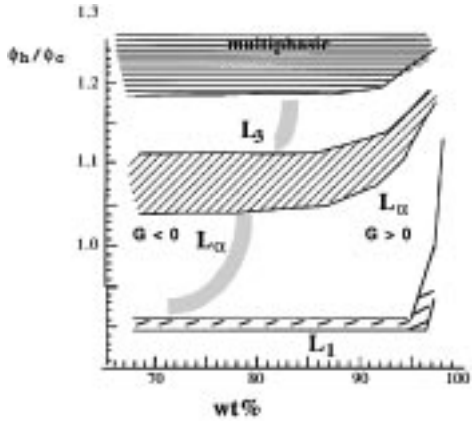

Figure 2. Phase diagram of the system studied: simplified sketch, adapted from ref. [1].

oily streaks and FCD's are observed at rest [4]. Ensembles of relatively monodispersed multilayered spherulites under shear have already been reported [5], but the observation of other types of defects, and the existence of several types of defects in the same system, depending on dilution, is a new feature in lyotropics.

(c) The L_3 phase (sponge phase) displays two different rheological behaviors as a function of dilution [6]. In the dilute region the L_3 phase transforms under very low shear rates, typically $20\,s^{-1}$, into a lamellar phase labelled here L^*_α, above some critical shear rate $\omega_a \sim \phi_s^x$, $x \sim 2.5$. The successive states observed when shear is

increased (flow birefringence, transition region with coexistence of L_α^* and L_3, and L_α^*) have been studied using simultaneously rheooptical methods, *in situ* X ray scattering, and light microscopy observations [6]. The existence of the $L_3 \Rightarrow L_\alpha^*$ transition is still debated [7] in less dilute surfactants ($\phi_s > \phi_s^* \sim 0.15$), where it is not visible at very small shear rates.

These experimental results will be described in the following sections, and tentatively discussed in the framework of the current theory of membranes. This theory involves a *large scale* description in terms of the magnitudes of the elasticity moduli κ (bending modulus) and $\bar{\kappa}$ (saddle-splay modulus), and the consideration of the microscopic thermal *fluctuations* of the membranes. The large scale description suffices to understand at a phenomenological level the stability of the different phases L_1, L_α and L_3 and, in principle, the observed types of defects. Unfortunately very few measurements of κ and $\bar{\kappa}$ are available to test the theoretical predictions. Note furthermore that, since the *crossover* (not a phase transition) between the two regions recognized in the L_α and L_3 phases occurs at constant ϕ_h/ϕ_c values, it has to be explained with only the contribution of the variation of the volume fraction of solvent ϕ_s. There is then little doubt that it is necessary to consider the thermal fluctuations [8], how they vary with ϕ_s, and how they affect the renormalized values of κ and $\bar{\kappa}$ with ϕ_s.

2. Static observations of defects in the L_α phase

2.1 *Experimental results*

Defects in the CpCl–hexanol–brine system have been described in various articles [2]. We shall content ourselves with the following comments:

(a) In *polarizing light microscopy* one observes: (1) spherulites and elongated 'rugby ball' defects in the most dilute region [2, 9]; their size varies in the range of 1 μm to 10 μm, and the maximum size does not seem to depend on the sample thickness; (2) in the intermediate crossover region the simultaneous presence of FCD's and spherulites; (3) in the less dilute region Friedel's oily streaks – i.e. dislocations of giant Burgers vectors, split into FCD's [2].

(b) In *freeze-fractured specimens* [2b] one observes: (1) spherulites and elongated 'rugby ball' defects of submicron size in the most dilute region; (2) in the region of crossover the simultaneous presence of FCD's and spherulites, as well as a typical crumpling (crinkling) of the layers for the higher ϕ_h/ϕ_c ratios in this region; (3) we have not investigated the small scales in the less dilute region.

2.2 *Focal conic domains of positive and negative curvatures*

Whether the samples are more dilute or less dilute, the different observed defects can be explained in the same framework. In both cases the bilayers – the membranes-present in the regions pervaded by the defects, are folded into parallel surfaces, which minimize the compression energy of the bilayers. The difference consists in the sign of the Gaussian curvature $G = \sigma_1\sigma_2$ at all points of the surfaces (σ_1 and σ_2 are the principal curvatures).

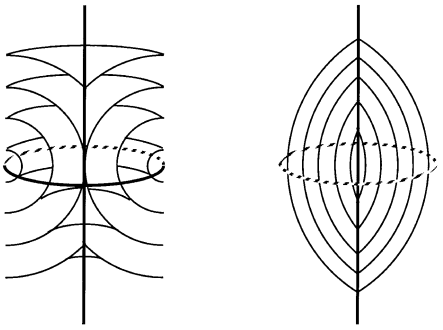

Figure 3. Focal conic domains with $G < 0$ and $G > 0$.

In the more dilute region all the surfaces have *positive* Gaussian curvature ($G \geq 0; G = 0$ in the free-defect regions), while in the less dilute samples one has *negative* Gaussian curvature ($G \leq 0; G = 0$ in the defect free regions). Both types of Gaussian curvatures are present in the crossover region. Because the compression energy per unit area $f_{\bar{B}} = d_\alpha/2\,\bar{B}((d - d_\alpha)/d_\alpha)^2$ is so small (it vanishes identically if the layers are parallel *and* situated at a distance d equal to the repeat distance d_α) the integral over the surface of all the bilayers $\int \mathrm{d}\Sigma d_\alpha \frac{1}{2}\bar{B}((d - d_\alpha)/d_\alpha)^2$ is negligible compared to the total curvature and saddle-splay contributions, whose free energy per unit area of membrane can be written as:

$$f_{\kappa\bar{\kappa}} = \tfrac{1}{2}\kappa(\sigma_1 + \sigma_2)^2 + \bar{\kappa}\sigma_1\sigma_2. \tag{1}$$

In this expression the $\bar{\kappa}$ contribution is of a pure topological nature: the quantity $\bar{\kappa}\int \mathrm{d}\Sigma\sigma_1\sigma_2 = \bar{\kappa}\int \mathrm{d}\Sigma G$ integrated over a surface does not vary if this surface is smoothly deformed. Therefore no principle of virtual work applies to this term, and $\bar{\kappa}$ can have any sign (on the contrary, κ is positive, necessarily). Therefore one expects that spherulites are favoured if $\bar{\kappa} < 0$, and conversely focal conic domains are favoured if $\bar{\kappa} > 0$.

Both types of defects are compatible with the symmetries of the lamellar phase and both minimize the elastic properties in a similar manner: they are all made of parallel bilayers and the singular parts of the packings are reduced to lines (figure 3). In both cases they deserve the name of focal conic domains (FCD's) – (FCD's of the first species, or FCD I, when $G < 0$; FCD's of the second species or FCD II in the opposite case). Onions (spherulites) are degenerate FCD II's, whose singularities are reduced to a point. Generic FCD II's possess a full line singularity (the hyperbola), while the ellipse is virtual.

FCD I's are common in thermotropic smectic phases, but in our system, FCD II's fill a larger part of the L_α region in the phase diagram than FCD I's.

3. Rheophysical properties of the L_3 and the L_3 phases

3.1 *The* $L_3 \Rightarrow L_\alpha$ *transition*

An $L_3 \Rightarrow L_\alpha$ transition under shear has long been suspected to exist [10] because of the large flow birefringence of the L_3 phase [11], but it is only recently that its existence [12]

has been clearly documented, first in our system [6a], and subsequently in pentaethyleneglycol *n*-dodecyl ether and susequently (C12E5) [13].

Birefringence measurements. Rheooptical measurements were made [6a, 14] in a range of applied controlled shear rates extending from $0.01\,s^{-1}$ to $450\,s^{-1}$. Birefringences Δn of the order of 5×10^{-9} could be measured since the noise is as low as 2×10^{-9}. The samples were all chosen along the same dilution line ($\phi_h/\phi_c = 1.15$) in the range $0.15 < \phi_s < 0.38$, and had values of ϕ_h/ϕ_c slightly decreasing, from 1.15 to 1.13, for smaller values of ϕ_s.

Again, the most interesting result is that the rheophysical behavior depends strikingly on the dilution: for the higher dilutions ($\phi_s < 0.13$), there is a remarkable transition to a lamellar phase at rather low values of the shear-rate (in the range $20\,s^{-1}$–$50\,s^{-1}$), while no transition is observed for the less dilute samples ($\phi_s > 0.15$), even for shear rates as high as $400\,s^{-1}$. These strikingly different behaviors occur in a system which does not show any brutal variation of its structural or transport properties (e.g. conductivity): it would be audacious to advance the idea that a phase transition occurs in the sponge phase in the $0.13 < \phi_s < 0.15$ composition range.

These results refer to a Couette cell geometry. The transition occurs through the following steps: first, below some shear rate ω_a, the sponge phase displays flow birefringence which increases practically linearly with the shear rate; then, in the range $\omega_a < \omega < \omega_c$, the system is biphasic, with the appearance of nuclei of a lamellar modification L_α^* which is oriented parallel to the shear plane (the so-called **a** orientation); finally, at $\omega > \omega_c$, the system transforms entirely to a lamellar phase, which is oriented parallel to the boundaries of the Couette cell (orientation **c**). In the more dilute part of the solvent range, viz. $0.05 < \phi_s < 0.15$ these results were corroborated by SAXS data collected during shear and optical observations just after shear and during relaxation.

For $\omega < \omega_a$, the birefringence shows the following behavior:

(a) At very small shear-rates, below some critical value ω_o, the birefringence Δn fluctuates in an erratic manner in the range $\sim 5 \times 10^{-9}$ to $\sim 2 \times 10^{-8}$, the extinction angle is at $\sim 45^\circ$ of the stream lines, and the scattered light intensity which is observed at the exit of the laser beam is small [6b, 14]. The values of ω_0 as functions of ω_s are reported in table 1 of ref. [6b]. Two regimes are clearly observed: ω_0 increases with ϕ_s increasing in the more dilute samples, and shows the opposite behavior for the less dilute samples.
(b) At higher shear rates, above ω_0, all the samples show linear flow birefringence $\Delta n = B_{\text{fl}}\,\omega$. Again, the values of B_{fl} display two regimes according to the range of dilution.

Characteristic times. All these results can be analysed [15] in terms of two characteristic times:

(a) *Short times* τ_r: According to Porte *et al* [16], there are two contributions to the shear birefringence in B_{fl}, one intrinsic and the other one due to the shape anisotropy, as follows:

$$\Delta n = B_{\text{fl}}\,\omega = (A\phi_s + B\phi_s^2)\tau_r\,\omega, \tag{2}$$

where A is the intrinsic contribution and B the shape contribution. In the sponge phase scaling regime [16], i.e. in the limit of infinite dilution, the relaxation time τ_r of

the textures induced by the shear, which appears in eq. (2), scales as $\tau_r \sim \phi_s^{-3}$. This scaling regime indeed corresponds experimentally to the dilute region; when $\phi_s^2 B_{\rm fl}$ is plotted as a function of ϕ_s in the corresponding range, one gets as expected, $\phi_s^2 B_{\rm fl} \sim A + B\phi_s + C\phi_s^3$, with $A/B \approx 1/10$, and C negligible: the shape birefringence is 10 times larger than the intrinsic birefringence. Extracting τ_r from eq. (2), one finds that the $\tau_r \sim \phi_s^{-3}$ law is well obeyed experimentally.

In the less dilute region the experimental data are at complete variance with those in the dilute region (see ref. [14]).

(b) *Long times* τ_b: the relaxation times of the birefringence in the range $\omega_a > \omega > \omega_o$ have also been measured, after cessation of shear. It appears that the relaxation can be described by a unique time τ_b, which takes the same values as $\tau_0 = 1/\omega$ when ϕ_s varies. These (long) relaxation times decrease with ϕ_s in the more dilute region and *increase* in the less dilute one.

Let us summarize the interpretation of the relaxation times in the more dilute region:

(a) The microscopic times τ_r occur in a range of shear-rates ($\omega > \omega_0$) too large to give time to a complete relaxation of the passages; they are therefore most probably related to the deformation by diffusion of the membranes (not to the relaxation of the passages), and equal to $\tau_1(q)$ for $q \sim 2\pi/d_3 \sim \phi_s$; with $\tau_1(q) \sim q^{-2}\phi_s^{-1}$. This expression yields a ϕ_s^{-3} scaling for τ_r as expected. Inserting experimental values for diffusivity [17], with $q^2 = 0.51 \times 10^{-10}\,{\rm cm}^{-2}$, $\phi_s = 0.053$, one gets $\tau_r(\phi_s = 0.15) \approx 2.5 \times 10^{-8}$ s i.e. of the right order of magnitude. This interpretation of the microscopic times in the more dilute region agrees with that of Diat and Roux [11] in another system (SDS, pentanol, dodecane, pure water.)

(b) The macroscopic times τ_b follow a scaling law quite different from the above for τ_r. Therefore it is not a single activated process which produces the difference between τ_b and τ_r, as proposed by Milner *et al* [18] and experimentally checked in ref. [11] (but again their system is different from ours). See also the last part of this paper.

The relaxation times in the less dilute region show a behaviour of a completely new type. If one assumes that the shape anisotropy is still predominant (eq. (2)), i.e. $B_{\rm fl} \sim \phi_s^2 \tau_r$ as in the dilute region, the experimental values of Δn yield a microscopic time $\tau_r \sim \phi_s^{-y}$; $y \sim 1 \pm 0.2$. As for the macroscopic time τ_b, it *increases* with ϕ_s.

3.2 *The lamellar phase*

We are currently investigating the steady-state rheological behaviour of the CPCl – hexanol – brine system along lines of dilution [4]. Here again (at $\phi_h/\phi_c = 1.025$) we distinguish experimentally two regions of dilution. In accordance with previous measurements in another lyotropic system [5], we obtain a power-law dependence of the viscosity as a function of the shear-rate ($\eta \sim \omega^{-m}$). In our case, $m \approx 0.9$ for $\phi_b > 0.77$, $m \approx 0.45$ for $\phi_b < 0.77$. The (dynamical) crossover at $\phi_b \approx 0.77$ seems to take place at a similar value of the dilution as the (static) crossover for defects. The value of m in the more dilute range, $m \approx 0.9$, is close to the value obtained in ref. [5], and the textures we observe under stationary shear (monodisperse spherulites) are of the same nature. But the rheological behavior in the less dilute range had not yet been documented in swollen lyotropic lamellar phases, to the best of our knowledge.

4. Theoretical analysis of membrane systems

The literature on the stability of the swollen phases has been the subject of a number of theoretical studies, none of them giving a completely satisfactory description of the observed L_1, L_α, and L_3 phases: whether they have a noticeably variable behavior with the composition of the membranes and/or the dilution, or not.

The nature of the crossover itself between the two regions is far from understood. In this paper we propose a very simple model for this crossover in the sponge phase. Previous models (Golubovic [19] or Morse [20]), which rely on an analysis of the length dependence of κ and $\bar{\kappa}$ via their logarithmic corrections[8], foresee the existence of several phases, of sponge and lamellar character, with passages, in the same system, as κ and $\bar{\kappa}$ are tuned by the variation in dilution. We do not need these logarithmic corrections to understand the *crossover* itself, but probably need them to understand the different nature of defects on each side of the crossover in the lamellar phase, as well as the possible variations of the structure of the sponge phase. Note incidentally that these corrections belong to a higher order of approximation (renormalization group) than the mean field approach developed in the sequel, which corresponds to a Gaussian approximation of the fluctuations.

4.1 *Plate elasticity and membrane elasticity*

Let us start by very simple considerations. The stability of the L_1, L_α, and L_3 phases can be discussed at a phenomenological level [21], starting from the surface free energy density of an isolated membrane (see eq. (1)). The result is as follows:

$$\begin{aligned}
&\text{for } 2\kappa + \bar{\kappa} > 0,\ \bar{\kappa} > 0 \text{ the sponge phase } L_3 \text{ is stable,}\\
&\text{for } 2\kappa + \bar{\kappa} > 0,\ \bar{\kappa} < 0 \text{ the lamellar phase } L_\alpha \text{ is stable,}\\
&\text{for } 2\kappa + \bar{\kappa} < 0,\ \bar{\kappa} < 0 \text{ the micellar phase } L_1 \text{ is stable.}
\end{aligned} \tag{3}$$

Note the similarity of eq. (1) with the classical free energy surface density of an inextensible solid plate [22]. The main differences between the 2 cases are: (1) the fact that the bilayer suffers considerable thermal fluctuations (κ is of the order of k_BT at room temperature), which have to be averaged out in this large-scale description [8]. Consequently the bending modulus κ and the saddle-splay modulus $\bar{\kappa}$ depend on some correlation length of the bilayer, which we shall denote as $\xi_\perp$ [23]. The bilayer is 'rigid' at short scales ($L < \xi_\perp$) and wrinkled at larger scales ($L > \xi_\perp$). Furthermore the integration $\int f \, \mathrm{d}\Sigma_p$ for the total energy is to be carried over a *mean surface* A_p averaged over the thermal fluctuations; (2) the inextensibility of the solid shell reduces the possible deformations of the shell to those which conserve lengths and angles, i.e. which conserve the Gaussian curvature G. The condition is less strict in a membrane; inextensibility is replaced by conservation of area. This being understood, the analogy is complete.

However this approach has clear limitations. No account is taken either of the interactions between neighboring membranes in eq. (1), or of the surface tension. The first point is well understood since Helfrich's [24] work, and will be briefly summarized, along with the discussion of thermodynamic fluctuations. The second one will be discussed in a forthcoming publication [25].

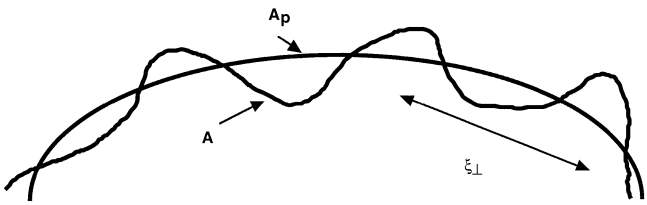

Figure 4. Averaged (Ap) and chemical (A) areas representing a membrane.

4.2 *Fluctuations of a free averaged membrane*

We start from well-known results [24]. Let A_p be the averaged area [26], A the true area, $\Delta A = A - A_p$ the excess area, of a membrane of typical size L. Let κ_0 be the so-called bare bending constant, related to a microscopic length a, typically the square root of the cross-section of a molecule of surfactant. The relative excess area can be written as

$$\frac{\Delta A}{A} = \frac{k_B T}{8\pi\kappa_0} \ln M, \tag{4}$$

where $M = A/a^2$ is the number of modes (figure 4).

Note that this expression is valid as long as A_p is smaller than $A_p^* = \xi_\perp^2$, since patches of size A_p^* are independent. Patches of area $A_p^* = \xi_\perp^2$ are indeed assumed to form a 2 dimensional ideal gas, of energy density $k_B T/A_p^*$. Another property of patches is that for $L < \xi_\perp$ the membrane behaves as a free membrane, while it is constrained at larger scales $L > \xi_\perp$.

Let δ be the thickness of a membrane (in this discussion the membrane is assumed to be incompressible; δ is a constant), and $\xi_\parallel$ the mean distance between bilayers. $\xi_\parallel$ is the repeat distance between bilayers: $\xi_\parallel = d_\alpha$ in the lamellar phase, and is equal to the correlation length $\xi_\parallel$ ($\xi_\perp = \xi_\parallel = d_3$) in the sponge phase, which is an isotropic liquid. We have

$$\phi_s = \frac{\delta A}{\xi_\parallel A_p}. \tag{5}$$

In this expression, $A_p > A_p^*$, necessarily. There is a natural crossover $A_p = A_p^*$. Comparing eq. (4) and (5) at the crossover, one gets

$$\phi_s \frac{\xi_\parallel}{\delta} = 1 + \frac{k_B T}{8\pi\kappa_0} \ln \frac{A^*}{a^2} = 1 + \frac{k_B T}{8\pi\kappa_0} \ln \phi_s \frac{\xi_\parallel}{\delta} \frac{A_p^*}{a^2}. \tag{6}$$

Using $A_p^* \approx \xi_\perp^2$, and expanding with respect to the (assumed) small parameter $\phi_s \xi_\parallel/\delta - 1$, one gets

$$\phi_s \frac{\xi_\parallel}{\delta} \approx \frac{1}{1 - k_B T/8\pi\kappa_0} \left(1 + \frac{k_B T}{8\pi\kappa_0} \ln \frac{\xi_\perp^2}{a^2}\right). \tag{7}$$

Equation (7) establishes a relationship between the concentration of surfactant and the mean distance between membranes, as soon as $\xi_\perp$ is known. Finally, since this theory of fluctuations is valid for $k_B T/8\pi\kappa_0 < 1$, we shall drop in the sequel the second order

terms, and write

$$\phi_s \frac{\xi_\parallel}{\delta} \approx 1 + c \tag{8}$$

with $c = c(\xi_\perp) = (k_B T/4\pi\kappa_0) \ln(\xi_\perp/a)$, a material constant of the membrane. Although eq. (8) is approximate, since it rests on the assumption that $A_p^* = A^*$, (c is not that small; however $k_B T/\kappa_0$ is smaller than unity in most of the experimental situations), we shall use it in the following.

4.3 *Large scale fluctuations $\xi_\perp$ in free and in constrained membranes: The crossover*

De Gennes and Taupin [27] have shown that a *free* membrane has a finite persistence length $\xi_\kappa = a \exp 4\pi\kappa_0/\alpha k_B T$. The value of the coefficient α varies according to different authors (Helfrich [28]: $\alpha = 1$; De Gennes and Taupin: $\alpha = 2$; Peliti and Leibler [29], Golubovic and Lubensky [30], David [31]: $\alpha = 3$). Assuming that a membrane has no interaction with neighboring membranes, i.e. in the limit of infinite dilution, we have, $\xi_\perp = \xi_\kappa$, i.e. $c(\xi_\kappa) = \alpha^{-1}$.

It is easy to show [24, 28] that the amplitude of the fluctuation of an element of membrane of size $A \approx \xi_\perp^2$ (we use the same approximation as above, and we assume $A \approx A_p$) scales as

$$\langle u^2 \rangle^{1/2} \sim \sqrt{\frac{k_B T}{\kappa_0}} \xi_\perp. \tag{9}$$

If the membrane is constrained by another membrane at a distance $\xi_\parallel$, one expects $\xi_\parallel \sim \langle u^2 \rangle^{1/2}$. Let $d_\parallel = \mu\sqrt{\kappa_0/k_B T}\xi_\parallel$, where μ is some constant of the order of $\sqrt{4\pi^3}$ according to Helfrich, then, using eq. (9), we get

$$\begin{aligned} &\text{if } d_\parallel \leq \xi_\kappa, \xi_\perp = d_\parallel; \\ &\text{if } d_\parallel > \xi_\kappa, \xi_\perp = \xi_\kappa; \end{aligned} \tag{10}$$

since $\xi_\perp$ is bounded from above by ξ_κ.

In the sponge phase, the critical ϕ_s^* of eq. (10) can be written as

$$\phi_s^* = \beta \frac{\delta}{\xi_\kappa} = (1 + c) \frac{\delta}{\xi_\kappa}, \tag{11}$$

where $\xi_\kappa = a \exp 4\pi\kappa_0/\alpha k_B T$ as above. In effect, the isotropy of the sponge phase yields $\xi_\perp = \xi_\parallel = d_3$, and eq. (8) can also be written as $\phi_s(\xi_\perp/\delta) \approx 1 + c$. In the sponge phase one gets experimentally $\beta \sim 1.4$, which suggests $\alpha \approx 2$. Taking $a = 4$ Å, $\delta = 30$ Å, and $\kappa_0/k_B T \approx 0.75$, one gets: $\phi_s^* \approx 0.114$, a value which fits reasonably well with our experimental critical value for the crossover in the sponge phase. But of course the result is very sensitive to very small changes in the material constants, because of the exponential behavior.

4.4 *Steric interaction of fluctuating membranes*

The free energy density (eq. (1)) has to be supplemented by the contribution of the repulsive forces due to the fluctuations which make the membranes to bump against each

other. This contribution is represented in the lamellar phases by the well-known Helfrich potential

$$V(\xi) = \beta \frac{(k_B T)^2}{\kappa_0 \xi^2}, \tag{12}$$

where ξ is the distance between neighboring averaged membranes, and $\beta = 3\pi^2/128$, according to Helfrich. The associated elastic modulus is

$$\bar{B} = \xi_{\|} \left. \frac{\partial^2 V(\xi)}{\partial \xi^2} \right|_{\xi=\xi_{\|}}. \tag{13}$$

5. Discussion

The above analysis of fluctuations has provided us with a reasonable argument for the existence of a crossover in the sponge phase. We have now to describe the structural and physical differences attached to this crossover in L_3, and the possible extension to L_α of arguments of a similar nature. Most of the proposals we make to this effect in the sequel are of a speculative and,hopefully, heuristic nature.

5.1 *Lamellar phase*

According to eq. (3), $\bar{\kappa} < 0, 2\kappa + \bar{\kappa} > 0$, in the L_α phase. These conditions are obtained under the assumption that the Helfrich steric contribution $\bar{B}$ is vanishingly small. The Helfrich contribution is certainly small in the more dilute region, but this is not so in the less dilute one, so that these conditions are less strict for the larger ϕ_s. The observations reported in ref. [2] give a rough estimation of the ratio $\bar{\kappa}/\kappa$ in various regions of the L_α phase; they indicate that $2\kappa + \bar{\kappa}$ is small in the more dilute region, close to the $L_1 \Longleftrightarrow L_3$ transition, with $\bar{\kappa} < 0$, as expected, while $\bar{\kappa}$ is definitely positive in the less dilute region, near the $L_\alpha \Longleftrightarrow L_3$ transition. The energy of an isolated spherulite of radius R can be written as [32]

$$W_{\text{spher}} = 4\pi\chi R + c\sqrt{\kappa \bar{B}/d_\alpha} R^2, \tag{14}$$

where $\chi = (2\kappa + \bar{\kappa})/d_\alpha, c \approx \pi^2/4$, and the energy of a FCD I, with ellipse of eccentricity e and semimajor axis a, can be written as [32]

$$W_{\text{FCDI}} = -4\pi\chi a\kappa(e^2)(1-e^2) + c'\kappa(1-e^2)a/d_\alpha, \tag{15}$$

where $\kappa(x)$ is the complete elliptic integral of the first kind, and c' a numerical constant which includes the core energy. Therefore the positiveness of $2\kappa + \bar{\kappa}$ favours FCD I's over the whole L_α phase, while onions have lower energy in the more dilute region ($\bar{\kappa} < 0$) than in the less dilute one. This is indeed what one observes: at rest (a) FCD I's are present all over the range of compositions [33], although less frequent in the dilute region, (b) spherulites are present only in the more dilute region, which they eventually entirely fill *under shear*. Therefore their presence at rest has been attributed to small shear rates occurring during the equilibration of the sample, and attempts have been made to

make samples without any shear action [33]. Note that this partition of the defects seems to be related to a variation of κ and $\bar{\kappa}$ at constant ratio of ϕ_h/ϕ_c. The renormalization of κ and $\bar{\kappa}$ in ref. [31] indeed foresees an increase of $2\kappa + \bar{\kappa}$ with ϕ_s.

The crossover itself will be discussed in a forthcoming publication [25].

5.2 *Sponge phase*

The *more dilute region* shows properties typical of the scaling laws of ref. [16], in particular the short relaxation times τ_r. As already stated, Diat *et al* [11] have found that the long relaxation times τ_b obey the same scaling law $\tau \sim \phi^{-3}$ as the short times, and are related by a Boltzmann factor

$$\tau_b = \tau_r \exp E/k_B T, \tag{16}$$

which indicates that an activated process separates the two phenomena. They attribute this process to a topological modification of the passages whose axis is perpendicular to shear, due to a merger of each such passage along its neck, whose effect is to create another passage rotated by a quarter turn (figure 5). Locally, the layers become parallel to the shear velocity.

The situation is obviously more complicated in our case, because the effect is not only local, but must encompass a transformation at a much larger scale, since eventually the L_3 phase transforms to the L_α phase. Therefore τ_b, while still the result of a unique relaxation process (there is only one relaxation time, experimentally), which is not described in ref. [17], probably deals with length scales much longer than d_3. Such a possibility is straight forward if the sponge phase is a lamellar phase disordered by dislocations, mostly of the *screw* dislocation type. That kind of model has many advantages: (a) the elastic energy is rather small (compared for example to *edge* dislocations [34]; also the elastic modulus $\bar{B}$ is

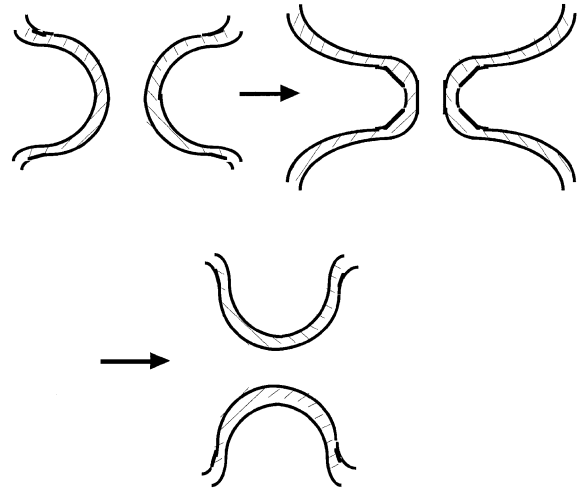

Figure 5. Topological disorientation of a passage under the action of shear (adapted from ref. [11]).

small, since $\xi_{\parallel} \geq \xi_{\perp}$ in the dilute region), (b) the membrane surfaces are close to minimal surfaces (and introduce as much negative Gaussian curvature as in the standard model of the sponge phase), (c) the entropy of disorder is as large as in the standard model. Hence the standard model of the sponge phase by Cates *et al* [35] should apply, provided there are as many dislocations of either sign, which is anyway to be expected. Furthermore the transition to a lamellar phase does not raise any serious topological problem, since the background is already lamellar.

It is more difficult to speculate about the *less* dilute region. The variation of the measured material constants with the dilution, which is at complete variance with what is observed in the dilute region, seems to indicate that the characteristic objects (passages?, screw dislocations?, disclinations?) are entangled. The model of minimal surfaces is probably less valid, because non-parallel neighboring membranes carry elastic (Helfrich) steric energy $\bar{B}$, which was negligible in the dilute region. The contribution of the topology to the free energy density $\int \mathrm{d}\Sigma \bar{\kappa} G = -4\pi\bar{\kappa}(N-1)(N \approx 1/\delta^3\phi_s^3$ is the number of passages per unit volume, plus the number of turns of screw dislocations of Burgers vector $\pm d_3$) is negative and may counter balance the steric term, and also the loss in entropy with respect to the dilute region. The intriguing possibility of the existence of disclinations is consistent with the importance of steric terms: remember that FCD's, which minimize steric energy, are particular forms of disclinations. If it is the case, then one might understand why the $\mathrm{L}_{\alpha} \Longrightarrow \mathrm{L}_3$ transition under shear is more difficult. Note however that the topological contribution already exists in the more dilute region. It would be useful to estimate quantitatively the role of the different terms in the two regions, but it is probable that, in the sponge case, as in the lamellar case, the renormalization of the curvature moduli plays a role.

Acknowledgments

The present paper borrows much from a common project with several collaborators, and includes experimental results obtained by Dr H F Mahjoub (PhD thesis). The author is particularly grateful to Sophie Asnacios, Claudie Bourgaux, Claire Meyer and Jean-Francois Tassin for helpful discussions and permission to quote unpublished results. Discussions with Christophe Blanc and Bernard D Coleman are also acknowledged.

References

[1] I Nastishin, E Lambert and P Boltenhagen, *Comptes-Rendus. Acad. Sci. Paris IIb.* **321**, 205 (1995)
[2] (a) P Boltenhagen, O D Lavrentovich and M Kleman, *J. Phys. II France* **1**, 1233 (1991)
(b) P Boltenhagen, M Kleman and O D Lavrentovich, *J. Phys. II France* **4**, 1439 (1994)
[3] G Friedel, *Ann. Phys. France* **2**, 273 (1922)
[4] C Meyer, S Asnacios, C Bourgaux and M Kleman, ILCC 17, Strasbourg 1998, in press
[5] O Diat and D Roux, *J. Phys. II France* **3**, 9 (1993)
T Gulik-Krzywicki, J C Dedieu, D Roux C Degert and R Laversanne, *Langmuir* **12**, 4668 (1996)
[6] (a) H F Mahjoub, K M McGrath and M Kleman, *Langmuir* **12**, 3131 (1996)
(b) H F Mahjoub, C Bourgaux, K McGrath J F Tassin and M Kleman, *Mat. Res. Soc. Symp. Proc.* **464**, 145 (1997)
(c) H F Mahjoub, C Bourgaux, P Sergot and M Kleman, *Phys. Rev. Lett.* **81**, 2076 (1998)

[7] C Bourgaux, private communication
[8] For a review on fluctuations see e.g. *Statistical Mechanics of Membranes and Surfaces*, edited by D Nelson *et al* (World Scientific, Singapore, 1989). The main results of the renormalization group approach in the calculation of κ and $\bar{\kappa}$ have recently been challenged by Helfrich, *Eur. Phys. J.* **B1**, 481 (1998)
[9] P Boltenhagen, O D Lavrentovich and M Kleman, *Phys. Rev.* **A46**, R1743 (1992)
[10] P Snabre and G Porte, *Europhys. Lett.* **13**, 642 (1990)
[11] O Diat and D Roux *Langmuir* **11**, 1392 (1995)
[12] H Hoffmann, S Hoffmann, A Rauscher and J Kalus, *Progr. Coll. Polym. Sci.* **84**, 24 (1991)
[13] J Yamamoto and H Tanaka, *Phys. Rev. Lett.* **77**, 4390 (1996)
[14] H F Mahjoub, J F Tassin and M Kleman, in preparation
[15] The results which follow belong to H F Mahjoub, PhD Thesis (Universite Paris 6, 1998) (see ref. [14])
[16] G Porte, M Delsanti, I Billard, M Skouri, J Appell, J Marignan, and F J Debeauvais, *J. Phys. II France* **1**, 1101 (1991)
[17] G Waton and G Porte, *J. Phys. II France* **4**, 5152 (1993)
[18] S T Milner, M E Cates and D Roux, *J. Phys. (France)* **51**, 2629 (1990)
[19] L Golubovic, *Phys. Rev.* **E50**, 2419 (1994)
[20] D C Morse, *Phys. Rev.* **E50**, 2423 (1994)
[21] G Porte, J Appell, P Bassereau and J J Marignan, *J Phys. (France)* **50**, 285 (1989)
[22] S P Timoshenko, *Theory of Elastic Stability* (McGraw- Hill Book Cy, New York, 1961)
[23] We adopt the notation used by liquid crystals people, viz. $\xi_\perp$ for lengths measured parallel the surface of the membrane, $\xi_\parallel$ for lengths measured perpendicular to the membrane.
[24] W Helfrich and R M Servuss, *Il Nuovo Cimento.* **3D**, 137 (1984)
[25] B D Coleman and M Kleman, in preparation
[26] Also called the projected area, because this theoretical approach is valid for quasi-planar surfaces
[27] P G De Gennes and C Taupin *J. Phys. Chem.* **86**, 2294 (1982)
[28] W Helfrich, *Z Natur.* **33A**, 305 (1978)
[29] L Peliti and S Leibler, *Phys. Rev. Lett.* **54**, 1690 (1985)
[30] L Golubovic and T C Lubensky, *Phys. Rev.* **A41**, 4343 (1990)
[31] F David, in *Statistical Mechanics of Membranes and Surfaces* edited by D Nelson *et al* (World Scientific, Singapore, 1989) p. 157
[32] P Boltenhagen, M Kleman and O D Lavrentovich, in *Soft Order in Physical Systems* edited by Y Rabin and R Bruinsma (Plenum Press, New York, 1994) p. 5
[33] C Blanc, private communication
[34] M Kleman, *Philos. Mag.* **34**, 79 (1976)
[35] M E Cates, D Roux, D Andelman, S T Milner and S A Safran, *Europhys. Lett.* **5**, 733 (1988)